Indian Journal of Radio & Space Physics
Vol 45, March 2016, pp 30-40

Association between earthquake and equatorial waves in outgoing longwave radiation over South East Asia

Manohar Lal[1] & G J Bhagavathiammal[2,$,*]

[1]KSKGRL, Indian Institute of Geomagnetism, Allahabad 221 505, Uttar Pradesh, India

[2]Department of Medical Physics, Anna University, Chennai 600 025, Tamil Nadu, India

[$]E-mail: selvigjb@gmail.com

Received 20 August 2015; revised 18 March 2016; accepted 28 March 2016

In the present study, efforts have been made to correlate the equatorial waves in outgoing longwave radiation (OLR) and seismic activities in South East Asian region. The OLR data has been obtained from NOAA Climate Prediction Centre web site. The earthquake information has been obtained from United States Geological Survey (USGS) Earthquake Information Centre. This paper presents observations for few earthquakes, including the ones on 26 January 2001 at Bhuj, India and on 26 December 2004 at Sumatra, Indonesia. The normal days OLR has been compared to the OLR recorded during the seismic events. It has been observed that there is significant enhancement in OLR few days before the earthquake event. The Morlet 6.6 wavelet analysis shows the presence of equatorial waves in equatorial OLR for a period of about 6-16 days during and about 80 days before the earthquake. The OLR data is analysed in such a way that the other possible effects are minimized. The anomalous increase and presence of planetary waves before 80 days of seismic event shows great potential in providing early warning of a disastrous earthquake. It may be noted that these waves are generated only in the equatorial region irrespective of strong/severe earthquake location.

Keywords: Earthquake, Equatorial wave, Planetary wave, Outgoing longwave radiation (OLR), Seismic event

PACS Nos: 91.30.P-; 92.60.Kc; 93.30.Db; 91.30.Nw

1 Introduction

Outgoing longwave radiation (OLR) is the radiant energy or the radiative flux leaving the Earth atmosphere system in the infrared (IR) region of the electromagnetic spectrum in a very broad wavelength range of 4 - 100 μm. It is an important component in the Earth's total energy budget. OLR is sensitive to clouds and water vapour and to some extent to dust and other greenhouse gases in the atmosphere. The surface and vertical distribution of temperature and therefore, the circulation of the atmosphere is decided depending upon the difference between the net incoming solar radiation and OLR[1]. The estimation of planetary radiation budget by satellites started since the beginning of the environmental satellite programme in early 1960s, but was for limited periods depending upon the lifetime of those experimental satellites[2]. Although, somewhat longer direct measurement of the broadband radiation budget began with the launch of Nimbus 6 and 7, the operationally available longest series of satellite estimations of OLR started from the NOAA series of satellites[3,4] during early 1970s. OLR is widely used as a tool in numerous applications and one of them is equatorial waves[5-9].

Gorny *et al.*[10] first used the NOAA-AVHRR thermal data of middle Asia region to suggest that abnormal infrared radiation observed by meteorological satellites could be taken as an indicator of seismic activity. Through subsequent studies, pre-earthquake thermal anomaly was observed in case of many earthquakes that occurred in China, Japan[11-16], Italy[17-20], USA[21,22], India, Iran[23-25], etc. These studies were based on detection of satellite data-based enhanced land surface temperature. Ouzounov *et al.*[26] have also explored the possibility of using earth's outgoing longwave radiation (OLR) as an indicator of impending earthquake activity and have reported around 6–22 W m^{-2} rise in OLR values. OLR is the thermal radiation flux emergent from the top of atmosphere and connected with the earth atmosphere system in general and is influenced by temperature and humidity.

This paper presents observations for the few earthquakes in South East Asian region. In all cases, an enhanced thermal infrared (TIR) emission days

before the main shock is evidenced in anomalous OLR values. Further, the presence of equatorial waves in OLR has also been studied for few months as an earthquake precursor.

2 Data analysis and Methodology

2.1 OLR data

The OLR energy flux is characterized by a number of parameters, such as emission from the ground, atmosphere and clouds formation, which have been observed on the top of the atmosphere by National Oceanic and Atmosphere Administration (NOAA) satellites[27]. These OLR data have been recorded twice daily by the several polar-orbiting satellites for more than eight years, forming time series data across different periods of time along with the spatial coverage of the entire earth. The original OLR data are processed by the interpolation technique to minimize the distance in space or time over which the value is interpolated. The details of the interpolation technique have been given by Liebmann & Smith[28]. The NOAA Climate Prediction Centre web site (http://www.cdc.noaa.gov/) provides the daily and monthly OLR data. The OLR algorithm for analysing the Advanced Very High Resolution Radiometer (AVHRR) data is from Gruber & Krueger[29], and integrates infrared radiation data between 10 and 13 μm. These data are mainly sensitive to near surface and/or cloud temperatures. The present study includes analysis of OLR data used measurements from AVHRR polar orbiters NOAA satellite. The data used for this study are twice-daily means from the NOAA-14 and 16 satellites. Their spatial coverage is 2.5×2.5 degree (latitude by longitude) covering the area of 90°N–90°S and 0°E–360°E, forming time series data over the specified region in the required period. It is worthwhile to remove the non-seismic components and retain information about the earthquake. The non-seismic components include the temperature changes caused by rainfall, cold and heat flows, and annual variation of the basic temperature field.

2.2 Methodology

There are several methods to choose from the analysis of OLR data, including the method of difference value[30], the method of the Eddy field calculation mean[31,32], the wavelet time-frequency analysis method[33-35] and the method of std threshold[33]. The method of the wavelet time-frequency analysis is capable of providing the time and frequency information simultaneously, hence, giving a time-frequency representation of the signal that could detect the prominent OLR singularities, follow continuity both in space and time. This method is more effective and obvious to detect anomalies within OLR data related to earthquake, which is in good accordance with previous study[26]. In this paper, a comparative analysis using the Morlet 6.6 wavelet analysis (http://paos.colorado.edu/research/wavelets/) method is undertaken for the study. This method is used to detect singularities within the OLR data in time and space covering the selected earthquakes.

2.2.1 Method of wavelet maxima

The basic theory of wavelet analysis calculation based on wavelet maxima has been described earlier[36,37] and the detailed practical guide to wavelet analysis has been provided by Torrence, & Compo[38]. A new analysis is carried out in the present study by enlarging spatial extent of study area for studying association between seismic activity in the South East Asian region and equatorial waves

First, an analysis area is defined by taking into account the epicentre and equatorial region over the ocean for identification of equatorial waves. Figure 1 shows the epicentre of the Bhuj earthquake marked with a star. This has been obtained from USGS Earthquake Information Centre

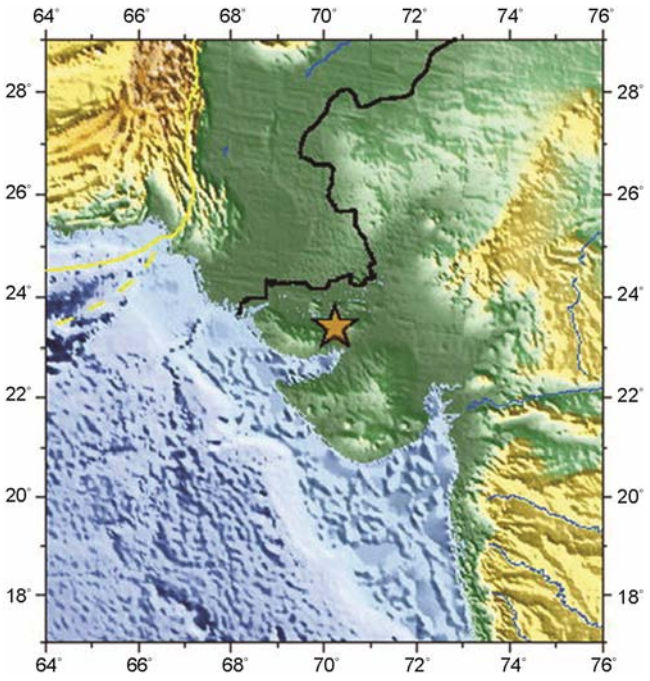

Fig. 1 — Epicentre of the Bhuj earthquake (on 26 Jan 2001 at 03:16:40 hrs UT, 23.41°N, 70.23°E, depth 16.0 km, magnitude 7.7) marked with a star [*Source*: USGS National Earthquake Information Centre]

(http://earthquake.usgs.gov/earthquakes/eqarchives/year/). An analysis area is defined and divided into a set of grids of 2.5×2.5 degree of latitude by longitude area over the epicentre. OLR data between 0°N - 30°N latitude and 60°E – 100°E longitude is used for the Bhuj earthquake analysis. Based on the defined grids, OLR daily data, from 1 January 2001 to 29 February 2001, is downloaded from the NOAA Climate Prediction Centre. The daily values of OLR have been considered for two months period prior to and after the earthquakes. The mean value during that period has been considered in order to take into account the seasonal effect. The monthly mean has been subtracted from the daily values to study the anomalous behaviour (ΔOLR) of OLR during the earthquakes and is shown in Fig. 2. This figure shows the daily value of OLR obtained over the Indian region. The upper portion of the graph is the Himalayan region and lower part is the Indian Ocean. The daily value of OLR has been subtracted from the mean monthly average for the identification of anomaly in OLR. Himalayan region shows the presence of lower values of OLR. On the other hand, OLR anomaly is significant in the Indian Ocean region (shown by the dark red contours).

Similarly, OLR monthly data for January months from 1995 to 2005 is downloaded from the NOAA Climate Prediction centre. The monthly values of OLR have been averaged for 10 years period prior to and after the earthquakes. The mean value of OLR has been considered for obtaining the anomalous changes (ΔOLR) in OLR during the earthquake months and is shown in Fig. 3. The data used for only January months minimises the effect of seasonal variation in meteorological parameter over the epicentre region.

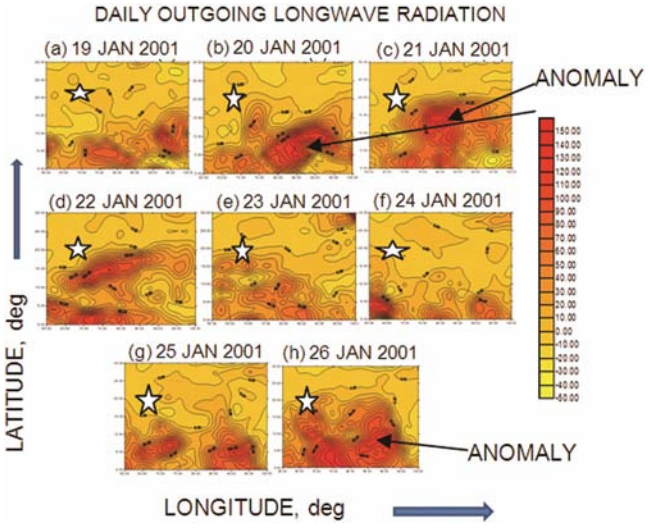

Fig. 2 — Longitude – latitude cross section of daily outgoing longwave radiation (OLR) contour over Indian region on: (a-h) 19 - 26 Jan 2001

The Morlet 6.6 wavelet method is employed to analyse the equatorial OLR data (10°S - 10°N latitude, 60°E – 100°E longitude) for identification of planetary scale equatorial wave during and before occurrence of severe earthquake in the South East Asian region (India, Pakistan, Indonesia, Myanmar, Afghanistan, Indian Ocean, etc.). Few cases of earthquakes are presented in the present study from the analysis of several events.

3 Results and Discussion

Generated OLR anomaly maps based on Advanced Very High Resolution Radiometer (AVHRR) data in case of South East Asian earthquakes produced meaningful information to correlate with the earthquake activity of the regions. Significant changes in OLR values has been observed over the Indian Ocean that remained responsible for generating possible linkage between equatorial waves in OLR and earthquakes of South East Asia. The significant earthquake events studied in the present case are shown in Tables 1 and 2.

A significant earthquake of magnitude 7.7 struck the Gujarat region, India on 26 January 2001 at 0847 hrs LT (0317 hrs UT) causing severe injuries and damage in the Bhuj-Ahmadabad-Rajkot area and other parts of Gujarat. The earthquake was felt throughout northern India and much of Pakistan, also felt in Bangladesh and western Nepal. The earthquake occurred along an approximately east-west trending thrust fault at shallow depth. The stress that caused this earthquake was due to the Indian plate pushing northward into the Eurasian plate. It was a

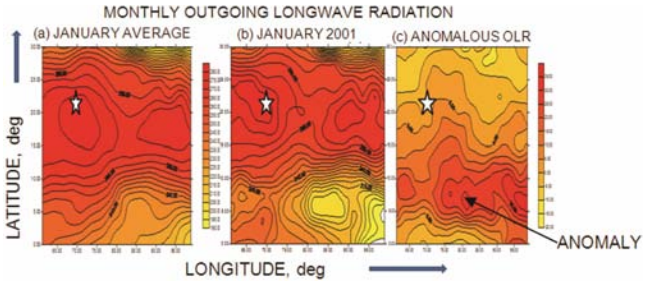

Fig. 3 — OLR reference field computed for: (a) monthly average of January using all available data between 1995 and 2005; (b) monthly average of January 2001 OLR contour considering epicentre and Indian Ocean region (0^{o}N-30^{o}N, 60^{o}E-100^{o}E); (c) anomaly obtained in the monthly average value of OLR (January average OLR – January 2001 OLR)

Table 1 — List of the earthquake events taken in the analysis and identified OLR anomalies

S No	Name	Date	Geographic lat/long	Monthly OLR anomaly time and location	Monthly OLR anomaly strength, Wm^{-2}	Daily OLR anomaly time and location	Daily OLR anomaly strength, Wm^{-2}	NOAA satellite
1.	Bhuj, Gujarat, India	26 Jan 2001	23.63°N/ 70.24°E	Jan 2001 5.0°N/85.0°E	35	21 Jan 2001 15.0°N/80.0°E	150	NOAA-14
2.	Sumatra Andman island, Northern Sumatra	26 Dec 2004	3.09°N/ 94.26°E	Dec 2004 5.0°N/90.0°E	20	17 Dec 2004 5.0°N/93.5°E	130	NOAA-16

Table 2 — List of the earthquake events in Indonesian sector and intensity

S No.	Name	Date	Intensity	Location
1.	Banda Sea	30 Aug 2011	M 6.8	6.4°S, 126.8°E
2.	Indonesia	5 Spt 2011	M 6.6	2.96°N, 97.9°E
3.	India-Nepal Border	18 Spt 2011	M 6.9	27.7°N, 88°E
4.	Sumatra	10 Jan 2012	M 7.2	2.45°N, 93.2°E
5.	Sumatra	11 Apr 2012	M 8.2	2.3°N, 93.1°E
6.	Indonesia	25 July 2012	M 6.4	2.7°N, 96.2°E
7.	Banda Sea	10 Dec 2012	M 7.1	6.5°S, 129.8°E
8.	Indonesia	06 Apr 2013	M 7.0	3.5°S, 138°E
9.	Indonesia	02 July 2013	M 6.1	4.6°N, 96.7°E

complex earthquake. A small event was followed by a larger one about 2 seconds later (*Source*: United States Geological Survey, National Earthquake Information Centre, Earthquake Archives, http://earthquake.usgs.gov/earthquakes/eqarchives/significant/sig_2001.php). All available NOAA-AVHRR OLR data from 1 January to 29 February 2001 were processed and analysed to prepare OLR time series contours. The OLR contour for the Indian region during earthquake period shows conspicuous rise in OLR conditions (Fig. 2). The OLR anomaly first appeared on 19 January 2001 and increases on 20 and 21 January 2001. The region attained maximum increase on 21 January 2001, i.e. 5 days before the earthquake. The anomalous area occurred south-east of the epicentre. The OLR anomaly survey for this area shows values as high as 150 Wm^{-2} south-east of Bhuj epicentre. After that, area showed continuous decreasing OLR anomaly till normalcy achieved. But significant increase in OLR anomaly was observed on earthquake day, i.e. 26 January 2001, and it was also significant in the equatorial region (0°N-10°N, 70°E-90°E).

Saraf & Choudhary[39] observed that south-west Gujarat started to show an increase in temperature on 14 January 2001 with respect to the surrounding region. Within a few days, due to the extension of cracks and probably with further release of entrapped gases, there was a spread and increase of the thermal anomaly. The area experiencing this anomaly had spread in a NW–SE direction. On 23 January 2001, an anomaly was developed within an area of around 300 km^2, SE of the 26 January 2001 earthquake epicentre. Succeeding this boost, the increase started to wane out, probably with the closing of micro-cracks after 23 January 2001, just three days before the earthquake of 26 January 2001. On 23 January, the temperature was at a maximum between 28°C and 31°C in the anomalous region (about 5–7°C higher than the normal temperature). On 28 January 2001, the anomaly disappeared and the region showed a normal temperature of 24°C.

Singh & Ouzounov[40] found no foreshocks on 26 January 2001 during a period of clear weather. The main stress was released along the Katrol Hill and Mainland faults, there were no surface ruptures. NOAA-17 OLR survey for November showed that the largest value of OLR in the vicinity of 67.57°E reached 288.8 Wm^{-2} close to the Bhuj epicenter (23.6°N, 69.8°E). This was the highest value of the OLR field. For January 2001, the OLR reference field showed increasing values in Northern India close to Himalayan Mountains, probably connected with the gas release enhancement and additional flux emission on the platform boundaries due to deformation change. They compared the reference field for December 1999 to 2001 for NOAA-14, by computing the daily zonal mean over the epicentre area (65°–75°E) with one-degree gridded OLR data. Three areas were identified as anomalies in the OLR field, starting on 20 December, 10 January and 21 December. The largest positive increase in the OLR field for December 1999 – January 2001 was over the epicentre area (23°N, 70°E) and occurred on 21 January, 5 days before the event with a value of +6 Wm^{-2}.

The NOAA-AVHRR OLR data was analyzed between 1995 and 2005. The OLR reference field was computed for monthly average of January using all available data between 1995 and 2005 [Fig. 3(a)]. The

monthly average of January 2001 OLR contours considering epicentre and Indian Ocean region (0°N-30°N, 60°E-100°E) is shown in Fig. 3(b). This figure shows the OLR decrease in the Indian Ocean (about 5°N, 85°E), from 230 Wm^{-2} to 190 Wm^{-2}. The anomaly obtained in the monthly average value of OLR (January average OLR – January 2001 OLR) is shown in Fig. 3(c). There is a clear development of OLR anomaly in the equatorial region by about 40 Wm^{-2} and it might be related with the Bhuj earthquake.

Equatorial waves are a transport mechanism for chemical species, energy and momentum. They are known to propagate vertically from the lower to the upper atmosphere[41]. An important class of equatorial waves are Rossby waves and normal modes with periods around 2, 5, 10 and 16 days (Refs 42,43). The vertical propagation of such wave leads to wave breaking at higher altitudes due to the decrease in air density, which in turn results in wave mean flow interaction that is known to be a major driver of atmospheric dynamics in the winter time middle atmosphere[44]. Such wave mean flow interaction can drastically alter the zonal mean flow, and is often characterized by high wave activity[45-47]. The Morlet 6.6 wavelet analysis was performed for characterizing the waves in equatorial OLR (10°S-10°N, 60°E-100°E) using daily average OLR data from October 2000 to March 2001, before and after Bhuj 2001 earthquake. Figure 4 shows the power spectral density of daily mean OLR for Bhuj earthquake period. The upper panel [Fig. 4(a)] shows the OLR daily mean obtained from 1 October 2000 to 31 March 2001. The lower panel [Fig. 4(b)] shows the wavelet power spectral density. The insignificant power present in the spectral density curve is covered by the mesh. This figure shows the prominent presence of planetary waves of period about six days during and 80 days before onset of Bhuj earthquake.

Figure 5 shows the epicentre of the Sumatra earthquake marked with a star (*Source*: USGS). The OLR data of10°S-20°N and 80°E-100°E is used and divided into a set of grids of 2.5×2.5 degree (latitude by longitude) area over the epicentre, for the Sumatra earthquake analysis. The daily mean OLR data from 1 December 2004 to 31 January 2005 was downloaded from the NOAA Climate Prediction Centre. The monthly mean is subtracted from the daily values for identification of anomalous OLR (ΔOLR) during the earthquake period and is shown in Fig. 6. This figure shows the daily average of OLR contour obtained from 17 December to 26 December 2004 covering the epicentre (3.3°N, 96°E). The epicentre is

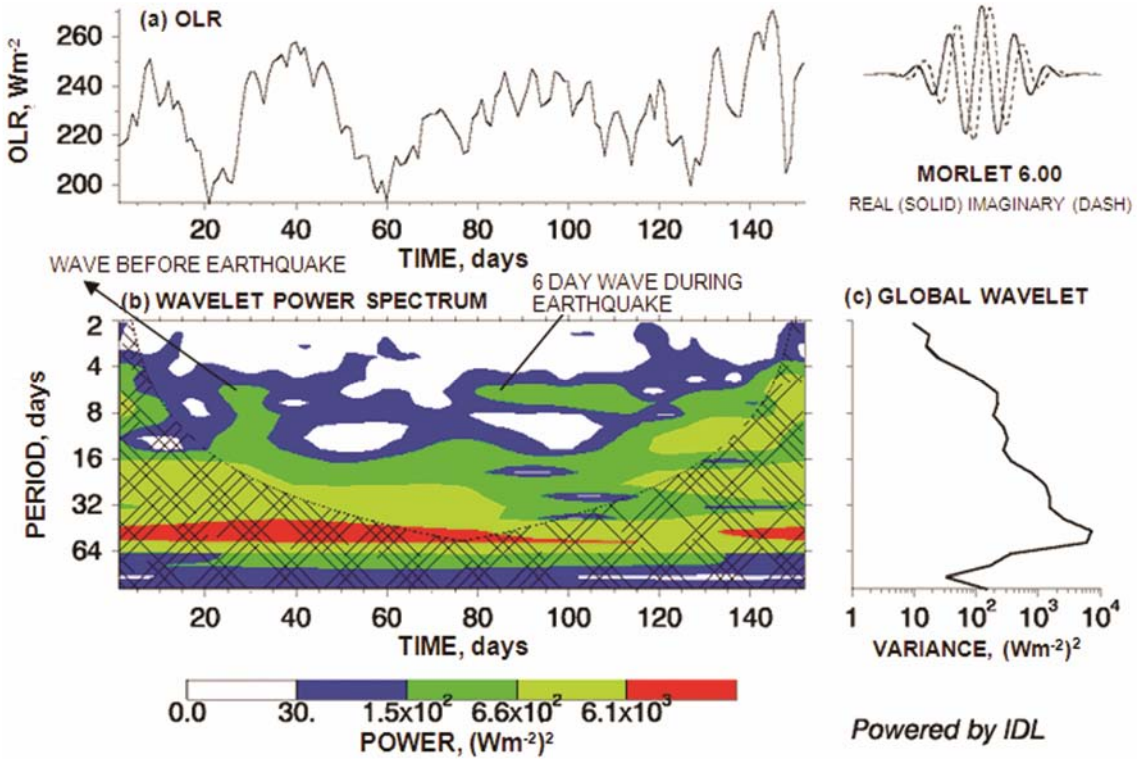

Fig. 4 — Power spectral density of daily mean OLR for Bhuj earthquake period: upper panel (a) OLR daily mean obtained from 1 Oct 2000 to 31 March 2001: lower panel (b) wavelet power spectral density using Morlet 6.6

shown as star in the figure. The anomaly present in the graph is shown by the arrow. The OLR anomaly developed at the epicentre on 17 December 2004 (nine days before earthquake) and started moving towards south-west and moved up to 22 December 2004 [Figs 6(h, g, f, e, d)]. Another anomaly in OLR is found on 24 December 2004, two days before earthquake, and this anomaly also shows south-west movement up to 26 December 2004, i.e. earthquake day [Figs 6(c, b, a)]. The OLR anomaly could be related to the Sumatra earthquake precursor.

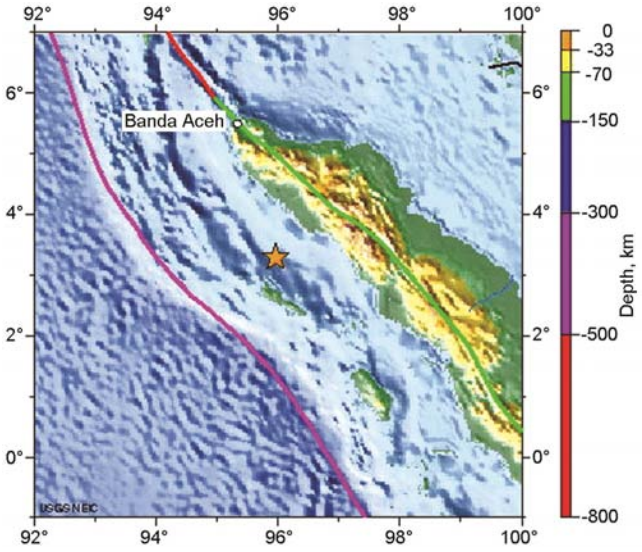

Fig. 5 — Epicentre of the Sumatra earthquake (on 26 Dec 2004 at 00:58:53 hrs UT, 03.30°N, 95.96°E, depth 30 km, magnitude 9.0) marked with a star [*Source*: USGS National Earthquake Information Centre]

The M9.0 Sumatra–Andaman Islands earthquake was the strongest and most devastating earthquake of the last forty years. Ouzounov *et al.*[26] used the NOAA IR daily data from NOAA-15 and monthly data from NOAA-17 to explore temporal and spatial variability of OLR prior to the 26 December earthquake. The maximum for the entire month in the area of 4°S–12°N, 8°–100°E is located at 4.5°N, 95°E and reached a value of +18.6 Wm^{-2}. A main OLR anomaly is offset from the Sumatra–Andaman Island region. Additional low OLR values dominating the epicentre area are found, which indicates coherence in temporal variability of low OLR field. They have calculated anomaly from December 2001 to 2004 and three areas were identified with potential anomaly values based on (Eq) for the OLR field starting on 20 October, 25 November and 22 December. They found largest ever-positive increase for the entire October 2001–December 2004 period in the OLR field over the epicentre area (3°N, 94.25°E) on 21 December.

OLR monthly data, for December months, from 2000 to 2010, downloaded from the NOAA Climate Prediction Centre, averaged for 10 years period prior to and after the earthquakes is shown in Fig. 7(a). The OLR contour has been obtained between 10°S to 20°N latitude and 80°E to 100°E longitude region. The monthly average of OLR obtained for December 2004 is shown in Fig. 7(b). The anomalous OLR (long term monthly average – December 2004) is shown in Fig. 7(c). This figure shows the anomalous OLR near to the epicentre (5°N, 90°E). The anomaly is found to be about 20 Wm^{-2}.

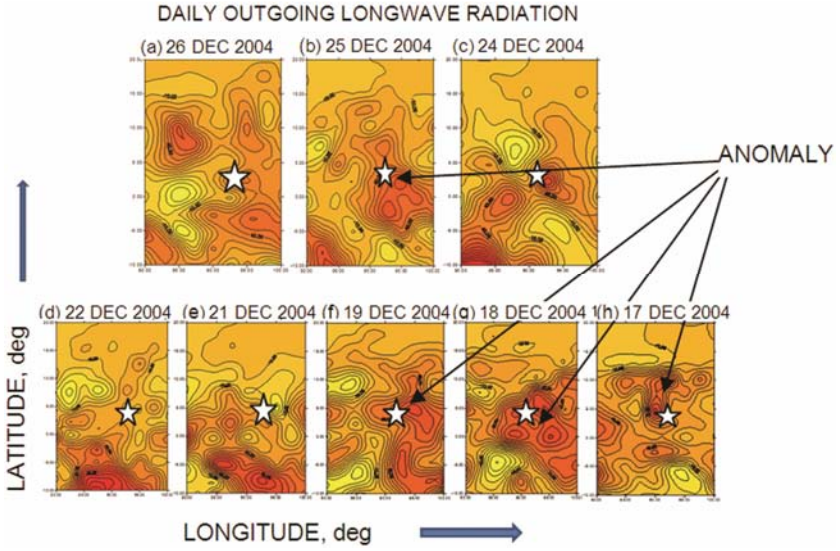

Fig. 6 — Longitude – latitude cross section of daily OLR OLR over Indian ocean on: (a-c) 26 – 24 Dec 2004; (d-e) 22 – 21 Dec 2004; and (f-h) 19 – 17 Dec 2004

The Morlet 6.6 wavelet analysis performed for the equatorial OLR data (10°S-10°N, 70°E-100°E), daily mean values, from September 2004 to January 2005, prior to and after earthquake, for identification of association between earthquake and equatorial waves is shown in Fig. 8. The upper panel [Fig. 8(a)] shows the OLR daily mean from 1 September 2004 to 31 January 2005. The lower panel [Fig. 8(b)] shows the wavelet power spectral density. The insignificant power present in the spectral density curve is covered by the mesh. This figure shows the presence of six days wave during the earthquake period (24 December 2004) and about 80 days before the Sumatra earthquake. More events are considered for the identification of empirical relation between equatorial wave and strong/severe earthquake in the South East Asian region. Figures 9-11 show the wavelet analysis of equatorial wave for 2011, 2012 and 2013, respectively. The wavelet spectrum has been obtained by taking daily average value of OLR between (10°S-10°N) and (60°E-100°E). One of the possible explanations for this relationship is the Lithosphere-Atmosphere-Ionosphere coupling mechanism[48,49], which provides the physical links between the different geochemical, atmospheric and ionospheric variations and tectonic activity. Briefly, the primary process is the ionization of the air produced by an increased emanation of radon (and other gases) from the Earth's crust in the vicinity of active fault[50-52]. The increased radon emanation launches the chain of physical processes, which leads to changes in the conductivity of the air and a latent heat release (increasing air temperature) due to water molecules attachment (condensation) to ions[53-55].

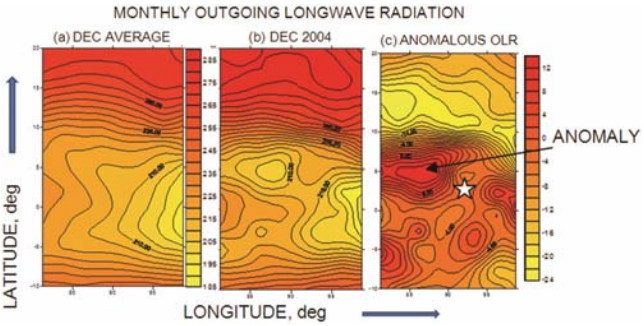

Fig. 7 —OLR reference field computed for: (a) monthly average of December using all available data between 2000 and 2010; (b) monthly average of December 2004 OLR contour considering epicentre and Indian Ocean region (0°N-30°N, 60°E-100°E); and (c) anomaly obtained in the monthly average value of OLR (December average OLR – December 2004 OLR)

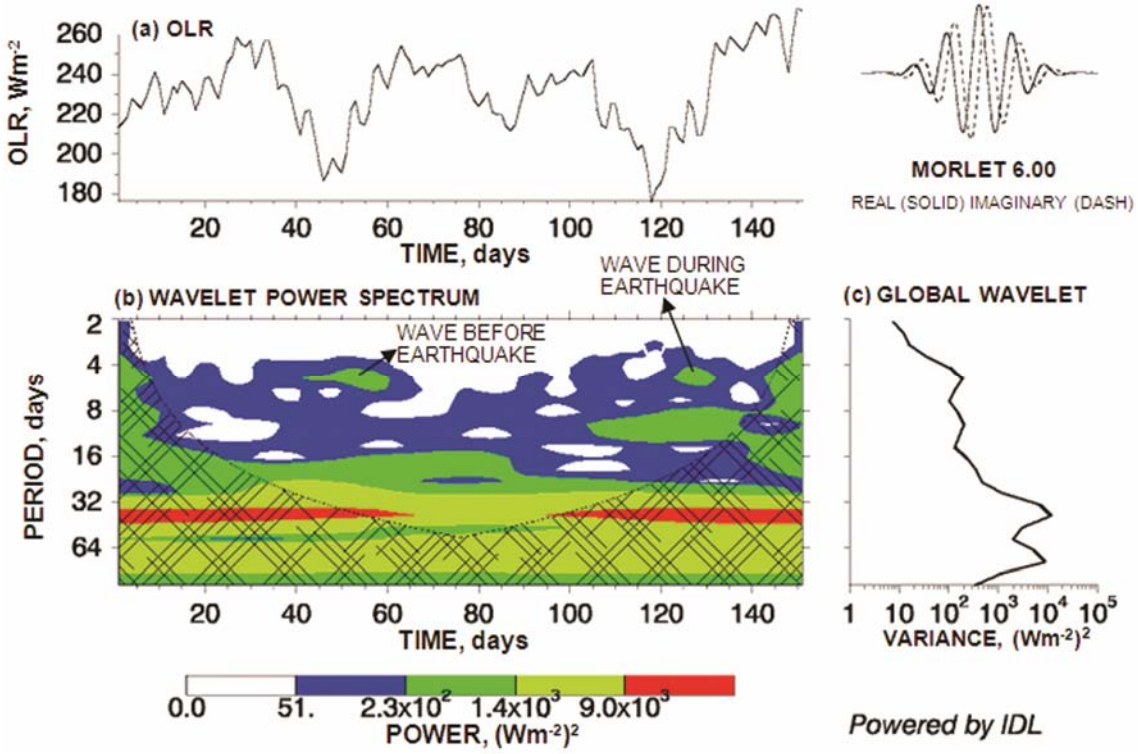

Fig. 8 — Power spectral density of daily mean OLR for Sumatra earthquake period: upper panel (a) OLR daily mean obtained from 1 Sep 2004 to 31 January 2005: lower panel (b) wavelet power spectral density using Morlet 6.6

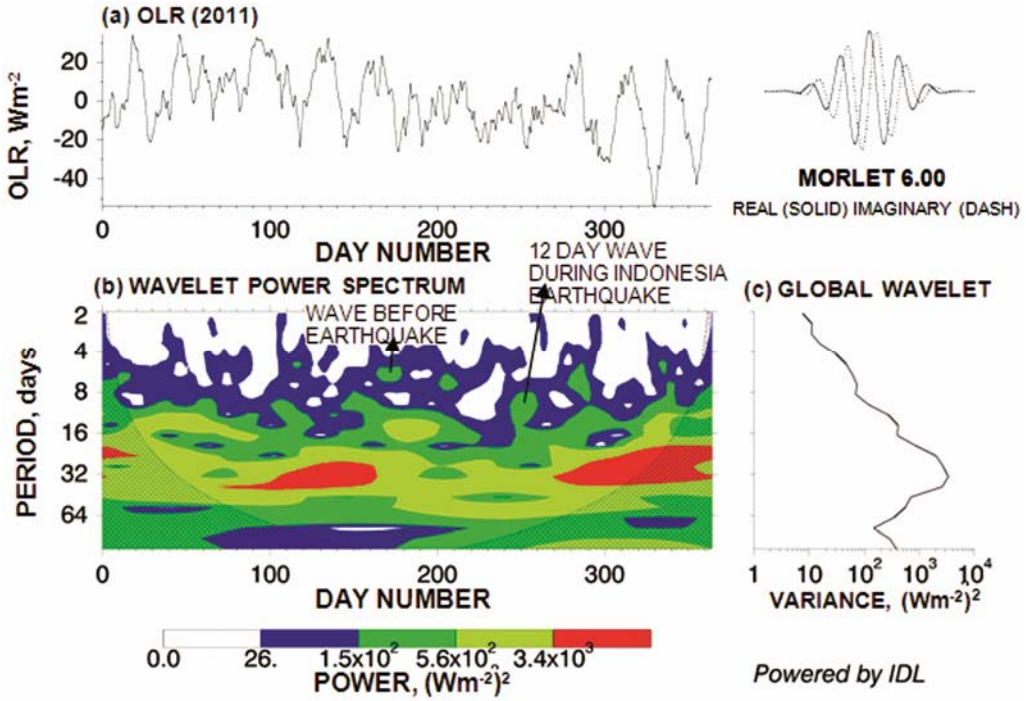

Fig. 9 — Power spectral density of daily mean OLR in Indian Ocean region for 2011: (upper panel) OLR daily mean obtained from 1 January to 31 December 2011; (lower panel) wavelet power spectral density using Morlet 6.6

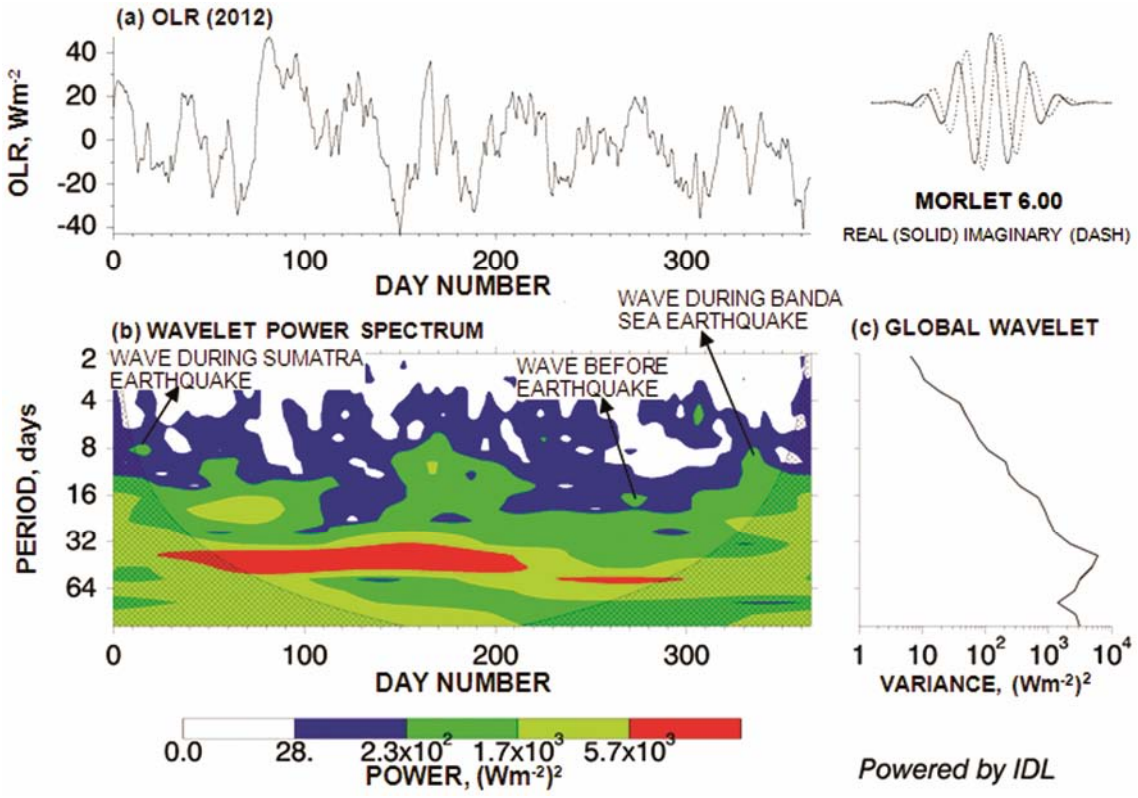

Fig. 10 — Power spectral density of daily mean OLR in Indian Ocean region for 2012: (upper panel) OLR daily mean obtained from 1 January to 31 December 2012; (lower panel) wavelet power spectral density using Morlet 6.6

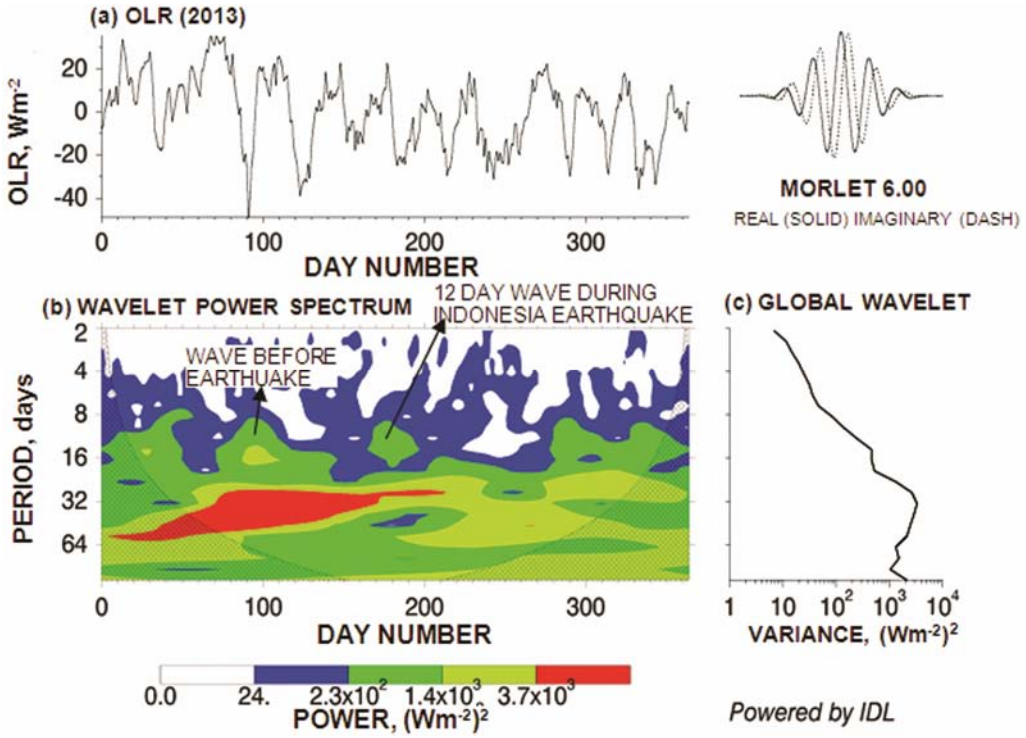

Fig. 11 — Power spectral density of daily mean OLR in Indian Ocean region for 2013: (upper panel) OLR daily mean obtained from 1 January to 31 December 2013; (lower pane) wavelet power spectral density using Morlet 6.6

There are several characteristics of the thermal anomaly, viz.: (i) thermal anomaly area and locations are quite different in size from event to event; and (ii) relationship between the anomaly and the earthquake magnitude is not clear. It may be associated with the geological setting, atmospheric environment and other conditions. Currently, deep study of the non-seismic factors is still lacking. It is difficult to determine the size and location of the earthquake by this method because of the complexity of geological, atmospheric and environmental conditions. Fortunately, there indeed exist thermal anomalies before major earthquakes. The thermal anomaly area is relatively large, at least tens of thousands of square kilometers before the earthquake. Therefore, to accurately determine the possible zone of future earthquakes, it requires not only use of the methods mentioned but also further analysis based on active tectonics.

4 Conclusion

The analysis of OLR data of the earthquakes has shown anomalous behaviour prior to the earthquakes. Such anomalous behaviour is found to be associated with the significant earthquakes of South East Asian region. The systematic pattern of OLR in the equatorial region shows a potential precursor to provide information about disastrous earthquakes occurring well in advance. The high resolution remote sensing data with better spatial and temporal resolutions may provide more reliable information about OLR, which can be easily used for early warning of significant earthquakes. In future, it is necessary to test the proposed methodology using more satellite data in order to investigate the possibility of improving signal-to-noise ratio among other improvements. Therefore, it is proposed that the KALPANA-1 satellite data may be utilised for the OLR studies over the South East Asian region. It is worth mentioning here that in the above analysis, the data is selected in such a way that the effect of diurnal, seasonal, latitudinal, longitudinal and altitudinal effects are minimized. At the same time, events were selected such that they were free from geomagnetic disturbed conditions, flares and thunderstorms. Thus, the OLR anomalies are directly related to the seismic events. The Morlet 6.6 wavelet analysis shows the presence of waves in equatorial OLR for a period of 6-16 days during and about 80 days before the earthquake. This shows that the

equatorial waves could be used as an earthquake precursor of South East Asian region. The anomalous increase and presence of planetary waves before 80 days of seismic event shows great potential in providing early warning of a disastrous earthquake. It may be noted that these waves are generated only in the equatorial region irrespective of strong/severe earthquake location.

Acknowledgement

One of the authors (ML) is thankful to his colleagues for valuable discussion. The authors are thankful to NOAA Climate Prediction Centre web site (http://www.cdc.noaa.gov/) for providing the daily and monthly OLR data. The authors are also thankful to United State Geological Survey (USGS) team for providing the information of seismic activity on their website http://earthquake.usgs.gov/activity/world.html. The Morlet 6.6 wavelet analysis (http://paos.colorado.edu/research/wavelets/) method was used for the present study for identification of planetary waves.

References

1 Mahakur M, Prabhu A, Sharma A K, Rao V R, Senroy S, Singh Randhir & Goswami B N, A high resolution outgoing longwave radiation dataset from Kalpana-1 satellite during 2004-2012, *Curr Sci (India)*, 105 (8) (2013) pp 1124-1133.

2 Suomi V E, The radiation balance of the Earth from a satellite, *Ann Geophys (France),* 6 (1957) pp 331-340.

3 Jacobowitz H W, Smith H L, Howell H B, Nagle F W & Hickey J R, The first 18 months of planetary radiation budget measurements from the Nimbus 6 ERB Experiment, *J Atmos Sci (USA)*, 36 (1979) pp 501-507.

4 Gruber A & Wintson J S, Earth-atmosphere radiative heating based on NOAA scanning radiometer measurements, *Bull Am Meteorol Soc (USA)*, 59 (1978), pp 1970-1973.

5 Lau K –M & Chan P H, Aspects of 40-50 day oscillation during summer as inferred from outgoing longwave radiation, *Mon Weather Rev (USA)*, 114 (1986) pp 1354-1369.

6 Hendon H H & Salby M L, The life cycle of the madden Julian oscillation, *J Atmos Sci (USA)*, 51 (15) (1994) pp 2225-2237.

7 Kiladis G N, Meehl G A & Weickmann K M, Large-scale circulation associated with westerly wind bursts and deep convection over the western equatorial Pacific, *J Geophys Res (USA)*, 99 (1994) pp 18,527-18,544.

8 Wheller M & Kiladis G N, Convectively coupled equatorial waves: Analysis of clouds and temperature in the wavenumber–frequency domain, *J Atmos Sci (USA)*, 56 (1999) pp 374-399.

9 Wheller M, Kiladis G N & Webseter P J, Large scale dynamical fields associated with convectively coupled equatorial waves, *J Atmos Sci (USA)*, 57 (2000) pp 613-640.

10 Gorny V I, Salman A G, Tronin A A & Shilin B B, The earth outgoing IR radiation as an indicator of seismic activity, *Proc Acad Sci USSR*, 301 (1988) pp 67-69.

11 Tronin A A, Satellite thermal survey – a new tool for the study of seismo active region, *Int J Remote Sens (UK),* 17 (1996) pp 1439-1455.

12 Tronin A A, *IGARSS*, Taking the pulse of the planet: the role of remote sensing in managing the environment, *IEEE 2000 International Geosciences Symposium* (IEEE, Honolulu, Hawaii), 2000, pp 2703-2705.

13 Tronin A A, Hayakawa M & Molchanov O A, Thermal IR satellite data application for earthquake research in Japan and China, *J Geodyn (Netherlands),* 33 (4-5) (2002) pp 519-534.

14 Qiang Z, Xiu-Deng X & Chang-Gong D, Thermal infrared anomaly-precursor of impending earthquakes, *Chin Sci Bull (China)*, 36 (4) (1991) pp 319-323.

15 Qiang Z, Kong L C, Zheng L Z, Guo M H, Wang G P & Zhao Y, An experimental study on temperature increasing mechanism of satellitic thermo-infrared, *Acta Seismol Sin (China),* 10 (2) (1997) pp 247-252.

16 Qiang Z, Chang-gong D, Lingzhi L, Min X, Fengsha G, Tao L, Yong Z & Manhong G, Satellite thermal infrared brightness temperature anomaly image-short term and impending earthquake precursors, *Sci China,* 42 (3) (1999) pp 313-324

17 Tramutoli V, Bello G Di, Pergola N & Piscitelli S, Robust satellite techniques for remote sensing of seismically active areas, *Ann Geofis (Italy),* 44 (2) **(**2001) pp 295 -312.

18 Tramutoli V, Cuomo V, Filizzola C, Pergola N & Pietrapertosa C, Assessing the potential of thermal infrared satellite surveys for monitoring seismically active areas: The case of Kocaeli (Izmit) earthquake, August 17, 1999, *Remote Sens Environ (USA),* 96 (3) (2005) pp 409-426.

19 Filizolla C, Pergola N, Pietrapersota C & Tramutoli A, Robust satellite techniques for seismically active areas monitoring: A sensitivity analysis on September 7, 1999 Athen's earthquake, *Phys Chem Earth (UK),* 29 (2004) pp 517-527.

20 Genzano N, Alianno C, Filizolla C, Pergola N &Tramutoli A, A robust satellite technique for monitoring seismically active areas: The case of Bhuj–Gujarat earthquake, *Tectonophysics (Netherlands),* 431 (1) (2007) pp 197-210.

21 Ouzounov D & Freund F, Mid-infrared emission prior to strong earthquakes analyzed by remote sensing data, *Adv Space Res (UK),* 33 (3) (2004) pp 268-273.

22 Ouzounov D, Bryant N, Thomas L, Pulinets S & Taylor P, Satellite thermal IR phenomena associated with some of the major earthquakes in 1999-2003, *Phys Chem Earth (UK),* 31 (2006) pp 154-163.

23 Saraf A K, Rawat V, Banerjee P**,** Choudhury S, Panda S K, Dasgupta S & Das J D, Satellite detection of earthquake thermal infrared precursors in Iran, *Nat Hazards (Netherlands),* 47 (1) (2008) pp 119-135, doi: 10.1007/s11069-007-9201-7.

24 Choudhury S, Dasgupta S, Saraf A K & Panda S, Remote sensing observations of pre-earthquake thermal anomalies in Iran, *Int J Remote Sens (UK),* 27 (18-20) (2006) pp 4381-4396.

25 Rawat V, Saraf A K, Das J D, Sharma K & Shujat Y, Anomalous land surface temperature and outgoing long-wave radiation observations prior to earthquakes in India and Romania, *Nat Hazards (Netherlands),* 56 (2011), doi: 10.1007/s11069-011-9736-5.

26 Ouzounov D, Defu L, Chun, K & Taylor P, Outgoing longwave radiation variability from IR satellite data prior to major earthquakes, *Tectonophysics (Netherlands),* 431 (1-4) (2007) pp 211-220.

27 NCAR and NOAA, NOAA *Interpolated Outgoing Longwave Radiation*, http:// www.esrl.noaa.gov/psd/data/gridded/data. interp OLR.html, 2008.

28 Liebmann B & Smith C A, Description of a complete (Interpolated) Outgoing Longwave Radiation Dataset, *Bull Am Meteorol Soc (USA),* 77 (1996) pp 1275-1277.

29 Gruber A & Krueger A F, The status of the NOAA Outgoing Longwave Radiation data set, *Bull Am Meteorol Soc (USA),* 65 **(**9) (1984) pp 958-952.

30 Kang Chun-li, Liu De-fu, Chen Yan & Zhou Xiao Cheng, Research on earthquake prediction method in North China using Outgoing Longwave Radiation Information, *Northwest Seismol J (China),* 28 (2006) pp 59-63.

31 Liu D F, Peng K & Liu W, Thermal omens before earthquake, *Acta Seismol Sin (China),* 12 (6) (1999) pp 710-715.

32 Liu D F, Anomalies analyses on satellite remote sensing OLR before Jiji earthquake of Taiwan Province, *Geo-Inform Sci (China),* 2 (1) (2000) 33.

33 Wang Y, Chen G & Kang C, Earthquake-related thermal infrared abnormity detection with wavelet packet decomposition, *Prog Geophys (China),* 23 (2) (2008) pp 368-374.

34 Xiong P, Bi Y & Shen X, A Wavelet-based method for detecting seismic anomalies in remote sensing satellite data, in *Machine Learning and Data Mining in Pattern Recognition* (Lecture Notes in Computer Science series, v 5632) (Springer Berlin Heidelberg), 2009a, pp 569-581.

35 Xiong P, Bi Y & Shen X, Study of Outgoing Longwave Radiation Anomalies Associated with two earthquakes in China using Wavelet Maxima, in *Hybrid Artifical Intelligence Systems* (Lecture Notes in Computer Science series, v 5572), (Springer Berlin Heidelberg), 2009b, pp 77–87.

36 Meyers S D, Kelly B G & O'Brien J J, An introduction to wavelet analysis in oceanography and meteorology: With application to the dispersion of Yanai waves, *Mon Weather Rev (USA),* 121 (10) (1993) pp 2858-2866.

37 Weng H & Lau K –M, Wavelets, period doubling, and time frequency localization with application to organization of convection over the tropical western pacific, *J Atmos Sci (USA),* 51(1994) pp 2523-2541.

38 Torrence C & Compo G P, A practical guide to wavelet analysis, *Bull Am Meteorol Soc (USA),* 79 (1998) pp 61-78.

39 Saraf A K & Choudhary S, NOAA-AVHRR detects thermal anomaly associated with 26 January, 2001 Bhuj earthquake, Gujarat, India, *Int J Rem Sensing (UK),* 26 (6) pp 1065-1073.

40 Singh R P & Ouzounov D, Earth processes in wake of Gujarat earthquake reviewed from space, *EOS Trans Am Geophys Unioin (USA),* 84 (2003), doi: 10.1029/2003EO260007.

41 Charney J G & Drazin P G, Propagation of planetary-scale disturbances from the lower into the upper atmosphere, *J Geophys Res (USA),* 66 (1961) pp 83-109.

42 Salby M L, Rossby normal modes in non-uniform background configurations, Part I: Simple fields, *J Atmos Sci (USA),* 38 (1981a) pp 1803–1826.

43 Salby M L, Rossby normal modes in non-uniform background configurations. Part II: Equinox and Solstice Conditions, *J Atmos Sci (USA),* 38 (1981b) pp 1827-1840, doi: 10.1175/1520-0469.

44 Andrews D G, Holton J R & Leovy C B, *Middle atmosphere dynamics* (Academic, San Diego, CA), 1987.

45 Hirota I, Kuroi K & Shiotani M, Mid-winter warmings in the southern hemisphere stratosphere in 1988, *Q J R Meteorol Soc (UK),* 116 (494) (1990) pp 929-941.

46 Sivjee G G, Walterscheid R L & McEwen D J, Planetary wave disturbances in the Arctic winter mesopause over Eureka (80^{o}N), *Planet Space Sci (UK),* 42 (1994) pp 973-986, doi: 10.1016/0032-0633(94)90057-4.

47 Jacobi C, Kürschner D, Muller H G, Pancheva D, Mitchell N J & Naujokat B, Response of the mesopause region dynamics to the February 2001 stratospheric warming, *J Atmos Sol-Terr Phy (UK),* 65 (2003) pp 843-855.

48 Pulinets S & Boyarchuk K, *Ionospheric precursors of earthquakes* (*Springer, Berlin),* 2004, 315.

49 Pulinets S & Ouzounov D, Lithosphere-Atmosphere-Ionosphere Coupling (LAIC) model - an unified concept for earthquake precursors validation, *J Asian Earth Sci (UK),* 41 (2011) pp 371-382.

50 Toutain J P & Baubron J C, Gas geochemistry and seismotectonics: A review, *Tectonophysics (Netherland*s), 304 (1998) pp 1-27.

51 Omori Y, Yasuoka Y, Nagahama H, Kawada Y, Ishikawa T, Tokonami S & Shinogi M, Anomalous radon emanation linked to preseismic electromagnetic phenomena, *Nat Hazard Earth Syst Sci (Germany),*7 (2007) pp 629-635.

52 Ondoh T, Investigation of precursory phenomena in the ionosphere, atmosphere and groundwater before large earthquakes of M > 6.5, *Adv Space Res (UK),* 43 (2009) pp 214-223.

53 Pulinets S, Kotsarenko A N, Ciraolo L & Pulinets I, A Special case of ionospheric day to-day variability associated with earthquake preparation, *Adv Space Res (UK),* 39 (2007) pp 970-977.

54 Cervone G, Maekawa S, Singh R P, Hayakawa M, Kafatos M & Shvets A, Surface latent heat flux and nighttime LF anomalies prior to the Mw=8.3 Tokachi-Oki earthquake, *Nat Hazard Earth Syst Sci.(Germany),* 6 (2006) pp 109-114.

55 Prasad B S N, Nagaraja T K, Chandrashekara M S, Paramesh L & Madhava M S, Diurnal and seasonal variations of radioactivity and electrical conductivity near the surface for a continental location Mysore, India, *Atmos Res(Netherlands),* 76 (2005) pp 65–77.